Applied Surface Science 329 (2015) 292–300

Contents lists available at ScienceDirect

Applied Surface Science

journal homepage: www.elsevier.com/locate/apsusc

Study on removal of elemental mercury from simulated flue gas over activated coke treated by acid

Jinfeng Ma[a,b], Caiting Li[a,b,*], Lingkui Zhao[a,b], Jie Zhang[a,b], Jingke Song[a,b], Guangming Zeng[a,b], Xunan Zhang[a,b], Yine Xie[a,b]

[a] College of Environmental Science and Engineering, Hunan University, Changsha 410082, China
[b] Key Laboratory of Environmental Biology and Pollution Control, Hunan University, Ministry of Education, Changsha 410082, China

ARTICLE INFO

Article history:
Received 22 May 2014
Received in revised form
14 November 2014
Accepted 18 November 2014
Available online 22 November 2014

Keywords:
Elemental mercury
Perchloric acid
Activated coke
Chemisorption
Flue gas

ABSTRACT

This work addressed the investigation of activated coke (AC) treated by acids. Effects of AC samples, modified by ether different acids (H_2SO_4, HNO_3 and $HClO_4$) or $HClO_4$ of varied concentrations, on Hg^0 removal were studied under simulated flue gas conditions. In addition, effects of reaction temperature and individual flue gas components including O_2, NO, SO_2 and H_2O were discussed. In the experiments, Brunauer–Emmett–Teller (BET), X-ray photoelectron spectroscopy (XPS) and Fourier transform infrared spectroscopy (FTIR) were applied to explore the surface properties of sorbents and possible mechanism of Hg^0 oxidation. Results showed that AC sample treated by $HClO_4$ of 4.5 mol/L exhibited maximum promotion of efficiency on Hg^0 removal at 160 °C. NO was proved to be positive in the removal of Hg^0. And SO_2 displayed varied impact in capturing Hg^0 due to the integrated reactions between SO_2 and modified AC. The addition of O_2 could improve the advancement further to some extent. Besides, the Hg^0 removal capacity had a slight declination when H_2O was added in gas flow. Based on the analysis of XPS and FTIR, the selected sample absorbed Hg^0 mostly in chemical way. The reaction mechanism, deduced from results of characterization and performance of AC samples, indicated that Hg^0 could firstly be absorbed on sorbent and then react with oxygen-containing (C—O) or chlorine-containing groups (C—Cl) on the surface of sorbent. And the products were mainly in forms of mercuric chloride ($HgCl_2$) and mercuric oxide (HgO).

1. Introduction

Mercury is known as an extremely hazardous substance because of its volatility, persistence and bioaccumulation. Methyl mercury, one organic transformation product of mercury, can be easily absorbed by human beings and have a hyper toxicity to nervous system [1,2]. The mercury in coal, in spite of its low concentration, is emitted directly and has become the major source of mercury in the atmosphere because of the large amount of coal burned. In order to prevent growing mercury pollution, "Minamata Convention on Mercury" was signed by 92 countries on 10 October 2013 to reduce the emissions of mercury and mercury compounds, while measures to control discharges from point source categories such as coal-fired power stations were put forward [3].

During the combustion, mercury is released into exhaust gas as elemental mercury (Hg^0) vapor, subsequently part of the vapor can be transformed into oxidized forms (Hg^{2+}) and particle-bound atoms (Hg^P) [4]. Commonly used air pollution control devices are effective for Hg^{2+} and Hg^P. For example, Hg^P can be easily removed through particulate matter (PM) control devices such as electrostatic precipitators (ESP) and fabric filters (FF). Water-soluble Hg^{2+} can be captured in wet flue gas desulfurization systems (WFGDs) with high efficiency [5–7]. Nevertheless, Hg^0 is difficult to be removed by using methods mentioned above because of its high volatility and nearly insolubility in water. Thus, exploitation of methods to capture Hg^0 is the key access to control the mercury emission [8].

Numerous technologies have been employed to remove elemental mercury from exhaust gas. Therein, activated carbon injection is widely adopted by coal-fired plants to control mercury emission. The carbon is injected into exhaust gas stream and recycled by ESP or in a baghouse [9]. In addition, activated carbons treated by metal oxides or chloride, such as TiO_2, $CuCl_2$, CeO_2, MnO_2, $CeCl_3$, V_2O_5, etc. [10–14], are extensively used in the

* Corresponding author at: College of Environmental Science and Engineering, Hunan University, Changsha 410082, China. Tel.: +86 731 88649216; fax: +86 731 88649216.
E-mail addresses: ctli@hnu.edu.cn, ctli3@yahoo.com (C. Li).

http://dx.doi.org/10.1016/j.apsusc.2014.11.090
0169-4332/

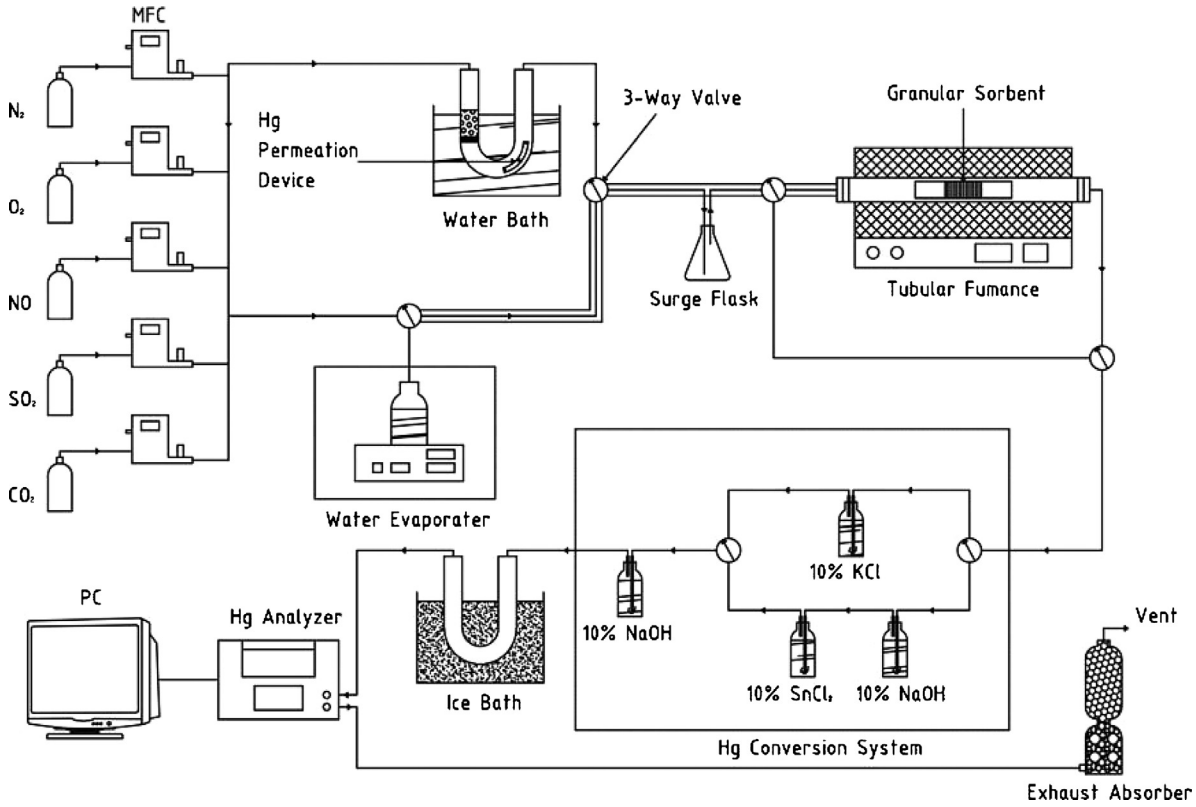

Fig. 1. Schematic diagram of the experimental setup.

process of Hg^0 settlement, in which Hg^0 is transformed into Hg^{2+} and then can be captured in WFGDs. However, these technologies cost tremendous capital, material and manpower, which hinders their wide applications. Besides, as an additive of concrete, the recycle activated carbon would cause secondary pollution due to Hg^0 release.

Activated coke (AC) is a kind of porous activated carbon-based adsorbent which is not adequately activated or retorting. Compared with activated carbon, AC possesses a higher mechanical strength and could be regenerated more conveniently. Furthermore, the price of AC is relatively inexpensive. Meanwhile, AC and activated carbon were similar in some aspects, such as the structure characteristics, adsorption and catalytic properties, physical and chemical stability [15]. In our previous studies [10,12,16], nitric acid (HNO_3) was used for pretreatment of catalysts. Oxidative acid could react with surface carbon-based substances and thus the structure of AC could be modified with the addition of oxygen-containing groups of acidic or alkaline which could improve the adsorption ability of sorbents. Additionally, massive researches indicated that chlorine played an important role in Hg^0 capture [12,17] since it could promote the conversion of Hg^0 to Hg^{2+} and Hg^{2+} was easy to be removed through solutions. Perchloric acid ($HClO_4$), the strongest inorganic acid, was widely used as oxidant in electropolishing and medical industry. Singh et al. [18] used $HClO_4$ to investigate the thermolysis of salts and demonstrated the oxidation through the reaction with ammonia. In this study, HNO_3, $HClO_4$ and sulfuric acid (H_2SO_4) were engaged into the activation on AC. Under simulated flue gases (SFG) conditions, the performance of modified AC on Hg^0 capture was evaluated through experiment in a tubular electric furnace. Various characterization methods were applied to study the structure and physicochemical properties of AC. Mechanism involved in Hg^0 oxidation was investigated as well.

2. Experiment

2.1. Samples preparation

The target sorbent in our study was a kind of standard commercial AC (columnar granules with a length of 7–9 mm and a diameter of 5 mm) made by Inner Mongolia Kexing Carbon Industry Limited Liability Company. Acid activated AC samples were prepared in steps as follow: at first, HNO_3, $HClO_4$, H_2SO_4 of 4.5 mol/L were added into beakers filled with AC granules, respectively. And the liquid–solid ratio was 2.5 ml/g. Secondly, $HClO_4$ treated AC sample series were produced in the same way as above, and the concentrations of $HClO_4$ varied from 1.5 mol/L to 7.5 mol/L. Then, all solid–liquid mixtures were stirred well and stood in darkness for 12 h. After acidification, all samples were washed by deionized water to neutral and dried in an electric blast oven at 95 °C for 6 h. Finally, the AC samples were cooled down to room temperature and stored in a desiccator. The HNO_3 treated sample was noted as AC_N as well as the H_2SO_4 treated sample was noted as AC_S. Moreover, the $HClO_4$ treated samples were noted as AC_X, where X (valued of 1.5, 3, 4.5, 6, 7.5) represented the molar concentration (mol/L) of $HClO_4$. Additionally, the blank sample was synthesized as a contrast following the methods above except for being immersed in deionized water, denoted as AC_F.

2.2. Experimental device and steps

The performance of acid activated AC was investigated on a bench-scale fixed bed system as shown in Fig. 1. All individual SFG components released from gas cylinders were controlled accurately by mass flow controllers. The rate of water vapor generated in evaporation plant was regulated by temperature controller. An elemental mercury permeation tube (VICI Metronics, USA) was

Table 1
Experimental setup and conditions.

	Sample	Carrier gas (720 ml/min)	Temperature (°C)
Set 1	AC_N, AC_S, $AC_{4.5}$ and fresh AC	SFG (5% O_2, 8% H_2O, 12% CO_2, 300 ppm NO, 500 ppm SO_2)	160
Set 2	AC_1, AC_3, $AC_{4.5}$, AC_6, $AC_{7.5}$	SFG (5% O_2, 8% H_2O, 12% CO_2, 300 ppm NO, 500 ppm SO_2)	160
Set 3	The optimal sample	SFG (5% O_2, 8% H_2O, 12% CO_2, 300 ppm NO, 500 ppm SO_2)	100–220
Set 4	The optimal sample	N_2/(N_2 + O_2) + individual flue gas components (NO and SO_2); SFG/SFG + 8% H_2O	The optimal reaction temperature

placed in a u-tube which was immersed in an electronic temperature water bath. After a period of balance at certain temperature, the Hg^0 permeation tube could emit stable Hg^0 vapor. All gas ingredients were well-mixed in a conical flask and then passed into the fixed-bed reactor, a tubular electric furnace coupled with a quartz tube with a length of 95 cm and an inner diameter of 52 mm. Before detected by mercury analyzer (Lumex RA-915M, Russia), gas mixture was dewatered in ice bath. Exhaust gas was introduced into an absorber filled with used AC and activated carbon before discharged into the atmosphere.

In this study, four sets of experiments were carried out and the details were listed in Table 1. Set 1 experiment aimed at screening the optimal acid used for treating AC sample. Performances of samples treated by different acids were evaluated under SFG (5% O_2, 8% H_2O, 12% CO_2, 300 ppm NO, 500 ppm SO_2, about 67 ng/L Hg^0 and balanced N_2) in the fixed-bed reactor. Total flow rate was set as 720 ml/min and the gas hourly space velocity (GHSV) was about 3000 h^{-1} employed in industry [19]. Hg^0 concentrations in outlet were recorded for 2 h to ensure data's stability. In Set 2, the effect of samples treated by optimal acid of varied concentrations (1.5 mol/L, 3 mol/L, 4.5 mol/L, 6 mol/L, 7.5 mol/L) on Hg^0 oxidation in SFG at 160 °C was designed to screen the optimal concentration. Set 3 experiments at each selected reaction temperature from 100 to 220 °C with an interval of 30 °C were designed to figure out the optimum reaction temperature in SFG. In Set 4, the roles of individual SFG components in Hg^0 removal and reaction pathways were explored in the presence of individual flue gases (balanced with N_2 or O_2 plus N_2) at optimal operating temperature.

In each test, when the goal temperature was reached, gas flow passed through the reactor for more than 20 min before recording data to ensure a stable Hg^0 feed concentration. A blank experiment was set up to check the mercury capture extent in gas system, including quartz tube reactor and glassware. And the result showed the efficiency on Hg^0 oxidation in blank test was fairly low which could be neglected. Considering the study of Hg^{2+} generated through oxidation and possible damage for detection cell of mercury analyzer by acidic gases, a mercury conversion system [8], described in the solid box of Fig. 1, was employed. In mercury conversion system, gas released from the reactor was firstly divided into two branches, one went to potassium chloride solution with a mass fraction of 10% which could remove Hg^{2+} for Hg^0 measurement, and the other went to stannous chloride solution to reduce Hg^{2+} to Hg^0 for total elemental mercury (Hg^T) measurement. Then the gas went through sodium hydroxide solution with a mass fraction of 10% to remove acidic gas. Supposing Hg absorbed on AC was mostly in oxidation state. Thence, the efficiency of Hg^0 removal (E_{oxi}) could be calculated by the formula below:

$$E_{oxi} = \frac{\Delta Hg^0}{Hg^0_{in}} = \frac{Hg^0_{in} - Hg^0_{out}}{Hg^0_{in}} \times 100\% \quad (1)$$

Hg^0_{in} and Hg^0_{out} stands for the Hg^0 concentration of inlet and outlet, respectively. Since the mercury discharged from reactor includes both Hg^0 and Hg^{2+}, mercury capture efficiency (E_{cap}) was introduced to evaluate the authentic performance of AC which was calculated as:

$$E_{cap} = \frac{\Delta Hg^0}{Hg^0_{in}} = \frac{Hg^0_{in} - Hg^0_{out}}{Hg^0_{in}} \times 100\% \quad (2)$$

where Hg^T_{out} represents the Hg^0 concentration at outlet of mercury conversion system after reducing action. It should be noted that Hg^T_{out} would not be less than Hg^0_{out} in this study.

Moreover, the standard deviation of data obtained from the test was delegated by error bars in following figures.

2.3. Characterization of catalysts

Brunauer–Emmett–Teller (BET) was performed by using a Tri-Star II 3020 analyzer (Micromeritics Instrument Corp., USA) to determine the specific surface area and porosity of samples. Every sample was dried at 105 °C overnight prior to BET measurement, and then degassed at 180 °C for 5 h under vacuum.

To identify the possible active groups and mercury species generated on sorbents, X-ray photoelectron spectroscopy (XPS) analysis was carried out on a K-Alpha 1063 analyzer (Thermo Fisher Scientific, USA) using 72 W Al Kα radiation from micro aggregation monochromator. The observed spectra were corrected with the C 1s binding energy (BE) value of 284.6 eV.

Fourier transform infrared spectroscopy (FTIR) was applied to this study with a SHIMADZU FTIR-8400S IRprestige-21apparatus. Its resolution factor was 2 cm^{-1} from 400 to 4000 cm^{-1} and scans were collected at a scan speed of 5 kHz. All samples to be tested were grinded and sieved to below 200 mesh before mixed with potassium bromide (spectral purity) and the mixture was tableted before been detected.

3. Results and discussion

3.1. Screening of optimal modified AC sample and temperature

3.1.1. Experiment for stability of sorbent

To ensure the reliability of data obtained from the test on sorbent performance under conditions of Set 1, experiment to investigate the stability of AC in Hg^0 removal was carried out. As shown in Fig. 2, the E_{oxi} of AC_F exhibited a descending trend from 86% at the beginning. After more than 17 h, the E_{oxi} was still staying above 69.74% which indicated that AC sample possessed excellent stablility in Hg^0 removal and could perform well in presupposed time quantum of 2 h for experiment.

3.1.2. Screening of acids

E_{oxi} over acid modified AC samples (AC_S, $AC_{4.5}$, AC_N) and AC_F were examined under conditions of Set 1, and the time-efficiency curves were shown in Fig. 3. Obviously, $AC_{4.5}$ and AC_N samples displayed higher properties in Hg^0 removal than AC_F through the 2 h test. In addition, AC_F performed better than AC_S in first hour and fell behind later. And the average Hg^0 removal efficiency of sorbents showed an ascending order: $AC_F < AC_S < AC_N < AC_{4.5}$. Compared to AC_F with the E_{oxi} of 74.05%, $AC_{4.5}$ obtained the highest E_{oxi} of 92.27% with a promotion of 18.22%, while the E_{oxi} of AC_N and AC_S increased by 7.4% and 0.55%, respectively. Singh et al. [18] suggested that the $HClO_4$ could decompose in a bimolecular process

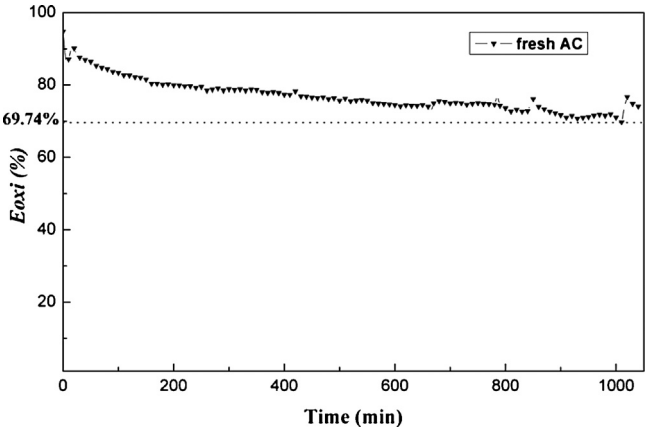

Fig. 2. Blank test on Hg^0 removal efficiency of AC_F. Reaction conditions: 160 °C; SFG (5% O_2, 8% H_2O, 12% CO_2, 300 ppm NO, 500 ppm SO_2, N_2 balanced); GHSV = 3000 h^{-1}.

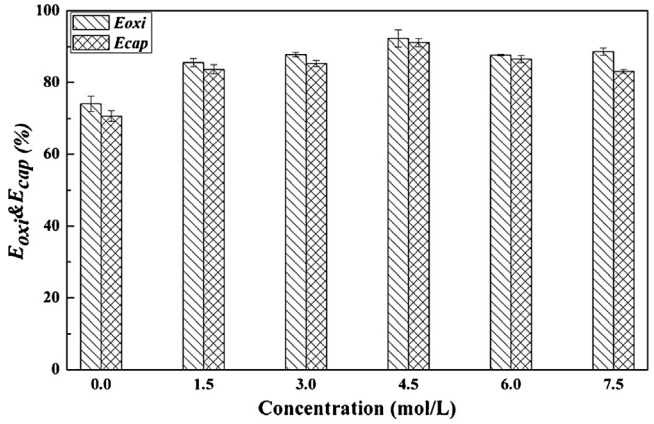

Fig. 4. Effect of acid concentrations on Hg^0 removal efficiency of AC treated by $HClO_4$. Reaction conditions: 160 °C; SFG (5% O_2, 8% H_2O, 12% CO_2, 300 ppm NO, 500 ppm SO_2, N_2 balanced); GHSV = 3000 h^{-1}.

giving the products of ClO_3 and ClO_4 and the generated chlorine oxides were of oxidability which w able to oxidize Hg^0. Another reaction between $HClO_4$ and carbon could produce Cl_2, the recognized as valid oxidant on Hg^0 [20]. The reactions could be expressed as followed:

$$7C + 4HClO_4 \rightarrow 2H_2O + 2Cl_2\uparrow + 7CO_2\uparrow \quad (3)$$

$$2HClO_4 \leftrightarrow H_2O + ClO_3 + ClO_4 \quad (4)$$

The deduction could be reached that the $HClO_4$ was able to bring about oxidants onto AC which would be responsible for the better performance of $AC_{4.5}$ in Hg^0 removal. It should be noted that the E_{oxi} was higher than E_{cap} of all AC samples, which was possibly caused by the loss of volatile product, such as mercuric nitrate.

3.1.3. Screening of acid concentrations

Fig. 4. presents the effect of $HClO_4$ concentration for modification on Hg^0 removal efficiency. The promotion of 21% at most and 13% at least in Hg^0 oxidation was observed over all modified samples compared with AC_F. Furthermore, the E_{oxi} and E_{cap} of the AC series got continuous improvement with the increasing acid concentration before 4.5 mol/L when $AC_{4.5}$ expressed the biggest E_{oxi} and E_{cap}, 92.27% and 91.12%, respectively. Considering the two reactions related to $HClO_4$ above, the improvement was believed to be due to the increasing amount of oxidizing groups emerged on the surface of AC samples while acid concentration increased.

When the acid concentration exceeded 4.5 mol/L, the averaged E_{oxi} and E_{cap} decreased. This result could not go on abiding by the aforesaid law between the acid concentration and the efficiency of Hg^0 removal. The discrepancy might be explained by the details found during the experiment: fragmentation happened in the process of performance test on AC_6 and $AC_{7.5}$. And the debris, moving along with the gas flow, of $AC_{7.5}$ was relatively more. It indicated that $HClO_4$ of high concentration would destroy the inside and outside structures of AC seriously and the weak mechanical strength of treated AC could not support the samples bearing long-playing heating and the crash of gas flow. Taking into account that the intact structure of sorbent was the foundation for efficient physisorption, the decline in E_{oxi} and E_{cap} of AC_6 and $AC_{7.5}$ was attributed to the suppression for physisorption by the broken structure of AC. That manifested that physisorption played some role in Hg^0 capture by AC.

Nevertheless, similar fragmentation was not observed in tests on other AC samples treated by lower concentrations. To sum it up, $AC_{4.5}$ was the sorbent performed best both in tests on different acids and $HClO_4$ concentrations, and the removal of Hg^0 was deduced as the synergy of physisorption and oxidation.

3.1.4. Screening of reaction temperatures

The performance of $AC_{4.5}$ on Hg^0 removal was investigated under conditions of Set 3 over the range of temperature from 100 to 220 °C, and the result was given in Fig. 5. It was apparent that when temperature rose from 100 to 160 °C, the averaged E_{oxi} and E_{cap}

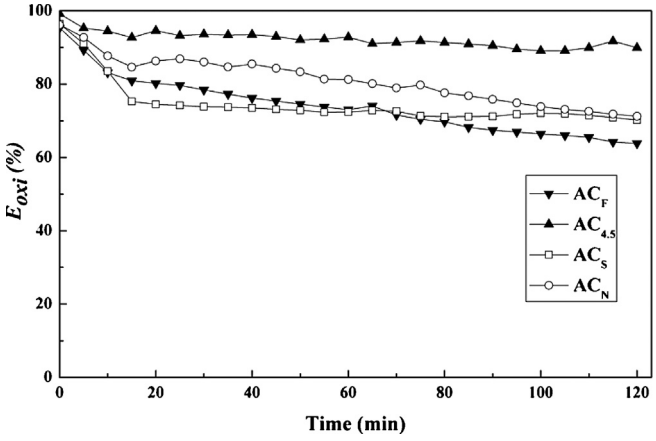

Fig. 3. Effect of different acids on Hg^0 removal efficiency of AC_N, AC_S, $AC_{4.5}$, AC_F. Reaction conditions: 160 °C; SFG (5% O_2, 8% H_2O, 12% CO_2, 300 ppm NO, 500 ppm SO_2, N_2 balanced); GHSV = 3000 h^{-1}.

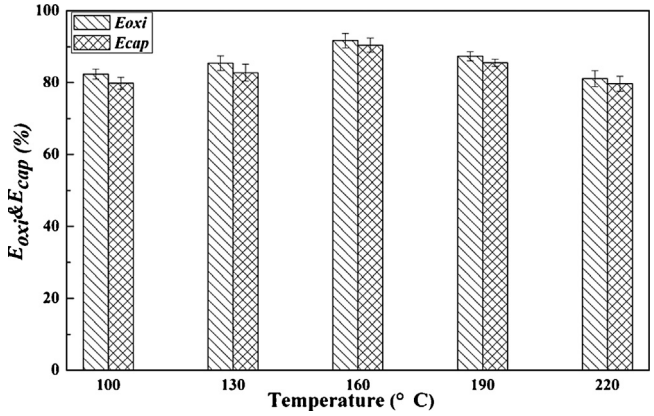

Fig. 5. Effect of temperature on Hg^0 removal efficiency of $AC_{4.5}$. Reaction conditions: 100~220 °C; SFG (5% O_2, 8% H_2O, 12% CO_2, 300 ppm NO, 500 ppm SO_2, N_2 balanced); GHSV = 3000 h^{-1}.

Table 2
BET surface areas and pore parameters of different catalysts.

Sample	Surface area (m^2/g)	Pore volume (cm^3/g)	Average pore size (nm)
AC	240.608	0.120420	2.00193
AC_S	211.454	0.106363	2.01203
AC_N	175.121	0.089242	2.03842
$AC_{4.5}$	110.036	0.063441	2.30619

increased from 82.35% and 79.80% to 91.67% and 90.45%, respectively. This demonstrated that the Hg^0 removal of $AC_{4.5}$ was mainly influenced by chemisorption cause the chemical reactions could be accelerated with the increase of temperature due to the catering for activation energy of reaction [12]. Nonetheless, the further increase of temperature over 160 °C led to a decrease in oxidative activity. When the temperature reached 220 °C, $AC_{4.5}$ showed E_{oxi} and E_{cap} of 81.08% and 79.70%, which were the lowest through the whole test. The decline of Hg^0 removal after 160 °C could be explained as follows: physisorption was inhibited due to Hg^0 adsorbed on $AC_{4.5}$ would volatilize at higher temperature; volatile mercuric compounds would be easier to sneak into gas flow and thus lowered E_{oxi} through the reduction in mercury conversion system; unstable mercuric compounds generated on $AC_{4.5}$ might decompose into Hg^0 and increase the Hg^0 concentration of outlet. Besides, according to previous literatures [21], the mercuric chloride producing reaction showed exothermic behavior, therefore the increasing temperature could hinder the reaction in which Hg^0 involved.

3.2. Characterization results

3.2.1. BET surface area analysis

Table 2 is the summary of the BET test for AC_F, AC_S, AC_N and $AC_{4.5}$. The results showed that the BET surface area of sorbents followed a descending order: $AC_F > AC_S > AC_N > AC_{4.5}$, which was also the same order for the total pore volume of samples mentioned above. Meantime, the average pore size of the stated sorbents showed the opposite tendency to the order of BET surface area and total volume of sorbents staying close to micro pore range (2 nm). It could be found that AC_F owned the biggest BET surface area of 240.6 m^2/g and total pore volume of 0.1204 cm^3/g, while the other samples were observed noticeable decrease in both surface areas and pore volumes through modification. Especially, $AC_{4.5}$ showed the distinctest change on sorbents' pore structure, which owned the smallest BET surface area (110.0 m^2/g) and total pore volume (0.0634 m^3/g) among all the sorbents. That was possibly resulted from the destruction of some of the thin pore walls on AC by strong oxidation of stated acids.

Compared with the order of BET surface area result, the sequence of performances in Hg^0 removal by stated samples was just opposite. It meant that $AC_{4.5}$, accompanied with the poorest BET surface area which was usually had a positive correlation with the efficiency of physisorption, performed best in Hg^0 removal. And thus the conclusion could be achieved that the chemisorption played dominant role in Hg^0 removal.

3.2.2. XPS analysis

High resolution XPS scans for selected elements (Hg 4f, Cl 2p, O 1s) were used to investigate the specific chemistry on selected samples (AC_F, fresh $AC_{4.5}$, used $AC_{4.5}$). And the result was shown in Fig. 6.

Fresh $AC_{4.5}$ was subjected to Hg^0 capture under the conditions of Set 1 for 12 h before XPS treatment. In Fig. 6A, the used $AC_{4.5}$ got a strong peak at 102.9 eV, ascribed to the Si 2p electron [22]. The spectrum of Hg captured showed two peaks at around 104.4 and 101.4 eV. The mercury and silicon profiles were obtained when the

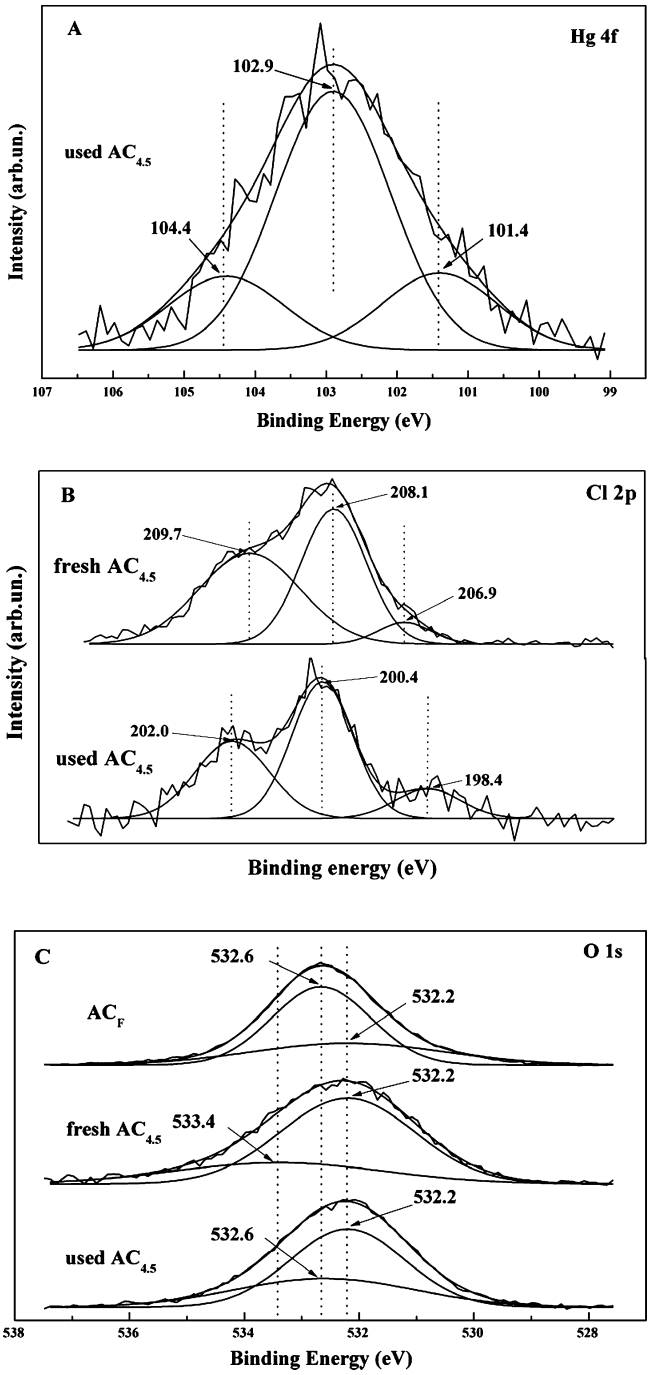

Fig. 6. XPS spectra of (A) Hg 4f of used $AC_{4.5}$; (B) Cl 2p of fresh and used $AC_{4.5}$ and (C) O 1s of fresh $AC_{4.5}$, used $AC_{4.5}$ and AC_F.

overlapped Hg 4f and Si 2p (SiO_2) signals were separated by peak fitting. The Hg $4f_{7/2}$ binding energy identified as 101.4 eV was distinctly higher than the 99.9 eV reported for Hg^0 [23]. It was believed that the result was attributed to the oxidation of elemental mercury, which was Hg^0 in the gas phase transformed into Hg^{2+} in the adsorbed phase. Based on the previously reported binding energy for Hg 4f on stated sorbent, the oxidation products of Hg^0 can be ascribed to HgO and $HgCl_2$ with two peaks located at 104.4 and 101.4 eV, respectively [22,24].

As shown in Fig. 6B for Cl 2p, three fitting peaks could be found in each spectrum of fresh $AC_{4.5}$ and used $AC_{4.5}$. After the comparison on relative positions of peaks in each spectrum, it could be observed that a significant migration occurred to the inferior

binding energy after Hg^0 removal. The peak of profile around 208.1 eV in spectrum of fresh $AC_{4.5}$ could be related to ClO_4^- type species [25]. Saraswat et al. [26] believed that $HClO_4$ was more rapidly ionized in acetonitrile and thus forced the polymer to release more and more electron to the cathode. It proved that $HClO_4$ possessed an excellent oxidizability and thus could perform well in Hg^0 oxidation.

In spectrum of used $AC_{4.5}$, the band of 198.4 eV corresponded to $HgCl_2$ in which chlorine was covalently bound to mercury [27]. Combined with the stated analysis about mercuric compounds, the formation of $HgCl_2$ during the process of mercury capture was confirmed. Moreover, it could be conjectured that the migration was possibly caused by the reaction between Hg^0 and chlorine-containing groups related to ClO_4^-.

The fitted O 1s XPS spectra for AC_F, fresh $AC_{4.5}$ and used $AC_{4.5}$ were presented in Fig. 6C. Comparing the binding energy scale of O 1s with relevant studies, the binding energy values of three different types of O 1s peaks could be used to judge the probably generated oxygen-containing groups. The O 1s peak appeared in spectra of all samples with the binding energy of 532.2 eV represented chemisorbed and/or weakly bonded oxygen (as in carbonyl or carboxyl groups), which were regarded as the most active oxygen in reaction of mercury oxidation [28,29]. The fitting peak of O 1s in region of 532.6 eV, corresponded to surface oxygen in hydroxyl species and/or adsorbed water species [30,31]. According to previous works, many hydroxyl groups were presented on the surface of AC [32]. The only emerged peak in profile of fresh $AC_{4.5}$, with a binding energy of 533.4 eV, was ascribed to ether-type oxygen [25]. Numerous recent studies shown that ether-type species, the primary product for carbonate-based electrolytes, was originated from reduction/reaction of the carbonate-based solvent [33,34].

Hypothetically, the atomic concentration of oxygen-containing groups corresponded to 532.2 eV and total oxygen on AC were denoted by O_A and O_T, respectively. After comparison of the profiles in used $AC_{4.5}$ with fresh $AC_{4.5}$ of O1s, it could be inferred that the increment in ratio (O_A/O_T) of effective oxidation groups increased from 35.26% to 72.47% was caused by the activation of $HClO_4$. The strong oxidation of $HClO_4$ and following pretreatment steps may be responsible for the variation between the peaks of 532.6 and 533.4 eV. Besides, it could be observed that the value of O_A/O_T decreased from 72.47% to 63.37% after Hg^0 removal. It clearly manifested that some chemisorbed oxygen was consumed when in experiment of removing Hg^0. United with the XPS result of Hg 4f, it could be verified that the HgO was the product of oxygen-containing groups and elemental mercury, both of which were absorbed weakly and adjacently on the surface of AC.

3.2.3. FTIR analysis

In order to investigate the changes in the surface groups associated with variations in the acidic/basic character of samples, FTIR characterization was carried out on all samples, including AC samples treated by different acids (AC_F, AC_S, AC_N, $AC_{4.5}$) and $HClO_4$ treated samples ($AC_{1.5}$, AC_3, $AC_{4.5}$, AC_6, $AC_{7.5}$). The FTIR spectra were recorded between 400 and 2000 cm^{-1}.

FTIR spectra of AC samples (AC_F, AC_S, AC_N, $AC_{4.5}$) were shown in Fig. 7. Similar profiles could be found in spectra of all the AC samples. The mutual peaks of AC_F at the bands of 1626, 1357 and 1000 cm^{-1}, which were corresponded to C=O vibration in carbonyl group, nitro (—NO_2) stretching vibration and SiO_4^{4-} stretching bands [35,36], respectively, were relatively weaker than those peaks of the modified samples. It demonstrated that the surface chemical properties of AC samples changed in the process of modification by acids. And the C=O groups were considered as positive in Hg^0 oxidation. What is more, the absorption band at 1390 cm^{-1}, assigned to the COO^- symmetric vibration, also showed

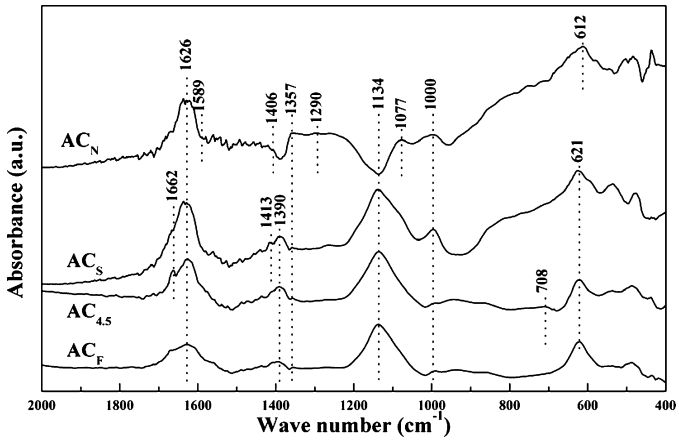

Fig. 7. FTIR spectra of AC_N, AC_S, $AC_{4.5}$, AC_F.

a sharppointed shape in spectra of AC_S and $AC_{4.5}$ rather than AC_F. Meanwhile, a concave emerged at the same band on the spectrum of AC_N with the peak located at 1357 cm^{-1} and new peaks appeared at the shoulders of the concave with the bands from 1406 to 1589 cm^{-1}, which were attributed to C=N vibrations and N—H bending vibrations. The same case took place at the band of 1134 cm^{-1} which was closely related to Si—O—C and new peaks at 1075 cm^{-1} (carbonate) and 1290 cm^{-1} (asymmetric stretching vibrations of C—O—C in ester groups) uprose [15,37,38].

Except the generated N-containing groups on AC_N, several kinds of functional groups closely bound up with properties of different acids emerged on other modified samples after modification. For instance, the bands at 1413 and 1662 cm^{-1} [39] were corresponded to S=O stretching vibration in curve of AC_S and C=O stretching vibration indicative of the carboxylic, anhydride or lactones in spectrum of $AC_{4.5}$, respectively. The description on efficient oxygen-containing groups was consistent with the correlative information in XPS analysis of O 1s, namely that chemisorbed oxygen existed on the stated four samples while the fresh $AC_{4.5}$ possessed more efficient oxygen than AC_F. Besides, the aromatic C—H group (708 cm^{-1}) [40] was only engendered on $AC_{4.5}$ which was conjectured to be intermediate product of activation. The bands of 612 cm^{-1} in curve of AC_N and 621 cm^{-1} in spectra of other three sorbents, attributed to SiO_4^{4-}, were detected [35]. That could be explained by the XPS result for Si 2p which indicated that a great amount of silicon belonged to AC. From the above, a conclusion could be reached that the treatment of acidification and oxidation by different acids brought numerous oxygen-containing functional groups, especially the activation of $HClO_4$, which brought additional oxygen.

As seen in Fig. 8, FTIR spectra of AC samples ($AC_{1.5}$, AC_3, $AC_{4.5}$, AC_6, $AC_{7.5}$) exhibited similar features with Fig. 7. The common peaks (at the bands of 1626, 1390, 1357, 621 and 1134 cm^{-1}) existed in most spectra of the sorbents tested by FTIR method. The similarities could be explained by the same raw material (AC) of all sorbents. The raw material was the mixture of diverse complex compounds, which contained groups corresponding to the mutual peaks by nature. Beyond that, peaks at bands of 1662 cm^{-1} (C=O stretching vibration) and 708 cm^{-1} (aromatic C—H group) which existed only in spectrum of $AC_{4.5}$ in Fig. 7 appeared in all curves of $HClO_4$ treated samples. It exactly indicated the groups of C=O (ascribed to the band of 1662 cm^{-1}) and aromatic C—H were the unique products of reaction between AC and $HClO_4$. The standpoint that the activation of $HClO_4$ could bring plentiful efficient oxygen-containing groups was proved again.

However, many differences could be observed among spectra of various samples. The peak of 1662 cm^{-1} got sharp gradually with

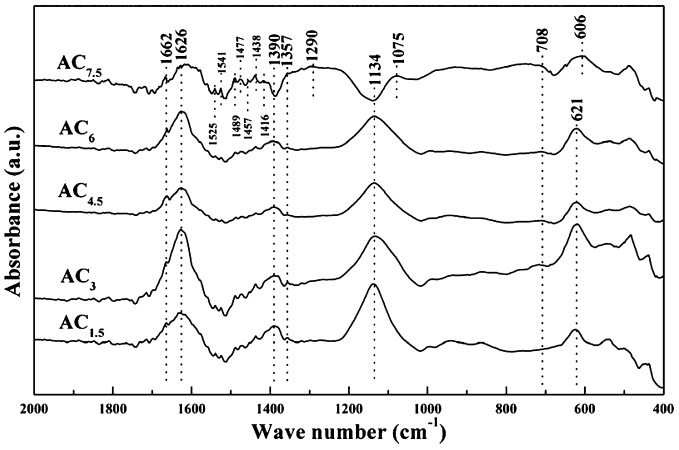

Fig. 8. FTIR spectra of $AC_{1.5}$, AC_3, $AC_{4.5}$, AC_6, $AC_{7.5}$.

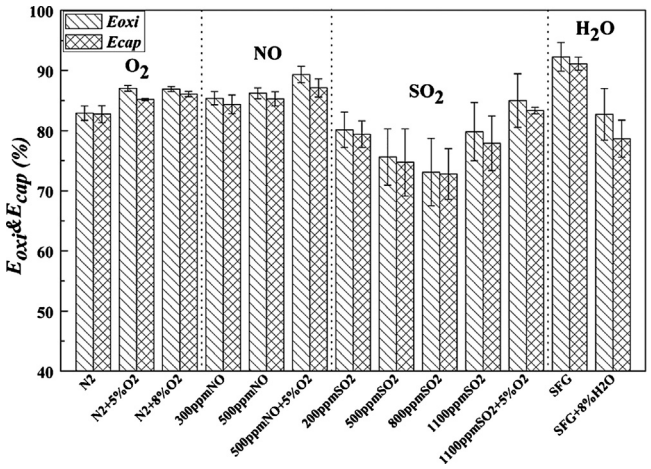

Fig. 9. Effect of individual flue gas component on Hg^0 removal efficiency of $AC_{4.5}$. Reaction conditions: 160 °C; $N_2/(N_2 + O_2)$ + individual flue gas components (NO and SO_2); SFG/SFG + 8% H_2O, N_2 balanced; GHSV = 3000 h^{-1}.

the increasing $HClO_4$ concentration. With a view of the decline in Hg^0 of AC_6 and $AC_{7.5}$, it could be affirmed that the chemisorption operated efficiently as usual while the fragmentation of AC resulted in seriously decreased pyhsisorption in Hg^0 removal, consequently, the fall in Hg^0 removal efficiency was expressed. Compared to AC samples treated by $HClO_4$ of lower concentration, peak of $AC_{7.5}$ at band of 606 cm^{-1} which was likely attributed to SiO_4^{4-} was regarded as the result of a slightly wavenumber excursion. Besides, a series of new peaks around 1416 and 1477 cm^{-1} (C=N vibration), 1438 cm^{-1} (—$CONH_2$ group), 1457 cm^{-1} (C—H deformation vibration), 1489 cm^{-1} (N—H bending vibration), 1525 and 1541 cm^{-1} (C=C vibrations in aromatics group) [36,41–44] appeared on the curve of $AC_{7.5}$, which were ascribed to the strong reaction of oxidation between $HClO_4$ and AC.

Striking resemblances in spectra of $AC_{7.5}$ and AC_N could be observed by the contrast between Fig. 7 and Fig. 8, especially the bands of concaves and newly emerged profiles. The coincidence could be interpreted as that the extents and abilities of modification by $AC_{7.5}$ and AC_N were similar; nitrogen-containing AC could produce compounds corresponded to certain FTIR wavenumbers under relevant extent of oxidation.

3.3. Effect of individual flue gas components

Individual flue gas components balanced in pure N_2 or N_2 plus O_2 were used to study their effect on Hg^0 removal under condition of Set 4 and the reaction pathways. The results are shown in Fig. 9.

3.3.1. Effect of O_2

E_{oxi} and E_{cap} over $AC_{4.5}$ at 160 °C under pure N_2 gas flow was observed to be 82.9% and 82.7%, respectively, which were clearly higher than those of AC_F under SFG condition. Considering the repeatedly validated deduction that oxidation played dominant role in Hg^0 removal. The capture of Hg^0 on $AC_{4.5}$ under pure N_2 atmosphere was mostly due to the reaction between Hg^0 and stored oxygen [8]. No obvious promotion of E_{oxi} and E_{cap} were detected when O_2 concentration ulteriorly increased to 8%. That indicated the modified $AC_{4.5}$ possessed an immense capacity for storing oxygen and the consumption of oxygen in oxidation during the experimental period was relatively little that the supplement for stored oxygen was unnecessary. Similar results were also obtained by other researchers [8,12].

3.3.2. Effect of NO

In the absence of O_2, E_{oxi} and E_{cap} of $AC_{4.5}$ were promoted to 85.38% and 84.36% when the concentration of NO was 300 ppm balanced with N_2 stream. Considering the surface chemisorbed oxygen, the NO could react in following steps to facilitate Hg^0 removal [8]:

$$NO + 1/2O_2 \rightarrow NO_2 \quad (5)$$

$$Hg^0 + NO_2 \rightarrow HgO + NO \quad (6)$$

$$Hg^0 + 2NO_2 + O_2 \rightarrow Hg(NO_3)_2 \quad (7)$$

With a melting point of 79 °C [45,46], $Hg(NO_3)_2$ was likely to volatilize at 160 °C. That could prove the existence of the volatile mercuric compounds which was mentioned earlier. Slight increase in Hg^0 removal could be found when higher concentration of NO was added. This demonstrated that the oxygen on sorbents was almost as effective as NO_2 for Hg^0 oxidation. As mentioned above, the modified $AC_{4.5}$ possessed an immense capacity for storing oxygen which could give the clue of the minor increase (3.1%) on Hg^0 oxidation efficiency after the addition of 5% O_2.

3.3.3. Effect of SO_2

Fig. 9 shows irregular situations of Hg^0 removal influenced by SO_2 of varied concentrations. Inhibition on E_{oxi} and E_{cap} of $AC_{4.5}$ sustained when concentration of SO_2 increased from 200 to 800 ppm, where the contribution of oxidation descended from 80.14% to 73.10%. It was possibly caused by the competitive adsorption between SO_2 and Hg^0 on the sorbent's active sites. However, the sudden positive effect for Hg^0 removal with the E_{oxi} and E_{cap} of 79.83% and 77.89% under 1100 ppm SO_2, respectively, was not conform to conventional studies [47,48]. Exceptionally, summarized from the discussions of Eric A. Morris and Qi Wan [49,50], SO_2 could react with functional groups on surface of AC. And the product, such as aromatic sulfide or sulfate species, could enhance the catalytic activation because of the newly formed sulfur-containing sites. That fitted the analysis of FTIR on the common peak (at band of 708 cm^{-1}) ascribed to aromatic C—H group in Fig. 8. Besides, the SO_2 absorbed on AC could react with the chemisorbed oxygen (O*) as equations below. And the SO_3, as a product, could oxidize Hg^0 to mercuric sulfate ($HgSO_4$) [51]:

$$SO_2(ad) + O* \rightarrow SO_3(ad) \quad (8)$$

$$Hg^0(ad) + SO_3(ad) + O* \rightarrow HgSO_4(ad) \quad (9)$$

Thus, the argument on the extraordinary performance of SO_2 on Hg^0 removal was deduced as follow: inhibition of competitive adsorption was not prominent in the atmosphere of SO_2 with a concentration of 200 ppm. In addition of the positive effect of sulfur-containing sites and SO_3, the slightly promotion in mercury

removal was expressed by $AC_{4.5}$ when compared with the efficiency of Hg^0 removal over AC_F; The impact of competitive adsorption deepened with the growing amount of SO_2 while improvement on Hg^0 removal efficiency by newly formed substances was correspondingly weak, hence a continued decline was manifested. When the concentration of SO_2 was 1100 ppm, the suppression caused by competitive adsorption between SO_2 and Hg^0 reached its limitation, and the subtotal active sites on AC were occupied by SO_2. As a consequence, the majority of chemisorbed oxygen that was able to oxidize Hg^0 before could only get in touch and react with SO_2, and more sulfur-containing sites and SO_3 were generated subsequently. Therefore, the reaction of Hg^0 oxidation was accelerated and introduced high E_{oxi} as well as E_{cap}.

When O_2 was added, E_{oxi} and E_{cap} of $AC_{4.5}$ got further improvement which might be due to the supplement of oxygen in active sites consumed by SO_2.

3.3.4. Effect of H_2O

Water-resistance is an important parameter to assess the application value of sorbent. In this test, 8% water vapor was added into simulated flue gas quantificationally and continuously. Hg^0 removal efficiency declined approximately 10%, shown in Fig. 9. The inhibition of H_2O might be explained mainly by the strongly competitive adsorption [52] and cover on catalyst surface by H_2O, and Hg^0 could not get in touch with active sites on the surface of sorbent. Thus both physisorption and chemisorption of Hg^0 were weaken.

3.4. The mechanism study

This study was conducted to figure out the actual behavior of $HClO_4$ acted in the process of Hg^0 removal. As above mentioned, $HClO_4$ could not only react with carbon to produce Cl_2, but decompose into ClO_3 and ClO_4 (denoted by ClO_x in union) at room temperature in Eqs. (3) and (4), respectively. Considering the deduction summerized from the analysis of FTIR and XPS on $AC_{4.5}$, which indicated that the modification by $HClO_4$ brought numerous efficient oxygen on AC, the possible reaction between ClO*x* and carbon over AC were proposed to be as follows:

$$ClO_x + (x+1)C \rightarrow xC{-}O* + C{-}Cl* \quad (10)$$

where Cl* represented chemisorbed chlorine. And the O* and Cl* could be replenished or regenerated by gas phase O_2 or Cl_2 in Eq. (11) and (12):

$$O_2 + C \rightarrow 2C{-}O* \quad (11)$$

$$Cl_2 + 2C \rightarrow 2C{-}Cl* \quad (12)$$

Considering the products, HgO and $HgCl_2$, generated in Hg^0 oxidation were proved to be subsistent from the analysis of XPS, the C—O* and C—Cl* were believed to played decisive roles in Hg^0 removal. Mechanisms involving atomic chlorine had been proposed by many researchers [8,12,20,53]. Eqs. (13)–(15) show the pathways, with Hg^0 was first absorbed on AC and then reacted with atomic chlorine:

$$Hg^0 + AC \rightarrow Hg(ad) \quad (13)$$

$$Hg(ad) + C{-}Cl* \rightarrow HgCl(ad) + C \quad (14)$$

$$HgCl(ad) + C{-}Cl* \rightarrow HgCl_2(ad) + C \quad (15)$$

Hg^0 oxidation by surface oxygen in AC was essential to Hg vapor capture. As seen in Fig. 9, satisfying E_{oxi} and E_{cap} were achieved over $AC_{4.5}$ at 160 °C under pure N_2 gas flow, demonstrating Hg^0 oxidation was mostly attributed to the reaction of chemisorbed oxygen with Hg^0 adsorbed adjacently. And similar conclusions had been drawn in numerous studies [39,47,51]. The reaction equation was described as follows:

$$C{-}O* + Hg(ad) \rightarrow HgO(ad) + C \quad (16)$$

4. Conclusions

$AC_{4.5}$ showed optimal E_{oxi} and E_{cap} in the tests for evaluation on activated coke treated by different acids and perchloric acid of varied concentrations. In addition, result of temperature experiment indicated that $AC_{4.5}$ performed best at 160 °C among the thermal gradient from 100 to 220 °C. The Hg^0 removal was the result of synergy between physisorption and chemisorption, and the latter one was attributed to the reaction between Hg^0 and Cl—O or C—Cl. Besides, the oxidation products, $HgCl_2$ and HgO, were further confirmed. Since the Hg^0 removal was a process which sostenuto consumed C—O and C—Cl, a further investigation to improve the regenerability of modified AC was needed.

Acknowledgements

This work is financially supported by the National Natural Science Foundation of China (51278177), the National High Technology Research and Development Program of China (863 Program, No. 2011AA060803) and the Scientific and Technological Major Special Project of Hunan Province in China (2010XK6003).

References

[1] S.X. Wang, L. Zhang, B. Zhao, Y. Meng, J.M. Hao, Mitigation potential of mercury emissions from coal-fired power plants in China, Energy Fuels 26 (2012) 4635–4642.
[2] H.F. Cheng, Y.A. Hu, Mercury in municipal solid waste in China and its control: a review, Environ. Sci. Technol. 46 (2011) 593–605.
[3] T.K. Mackey, J.T. Contreras, B.A. Liang, The Minamata convention on mercury: attempting to address the global controversy of dental amalgam use and mercury waste disposal, Sci. Total Environ. 472 (2014) 125–129.
[4] B.A. Dranga, L. Lazar, H. Koeser, Oxidation catalysts for elemental mercury in flue gases – a review, Catalysts 2 (2012) 139–170.
[5] R. Ochoa-Gonzalez, M. Diaz-Somoano, M.R. Martinez-Tarazona, The capture of oxidized mercury from simulated desulphurization aqueous solutions, J. Environ. Manag. 120 (2013) 55–60.
[6] S.S. Lee, J.Y. Lee, T.C. Keener, Novel sorbents for mercury emissions control from coal-fired power plants, J. Chin. Inst. Chem. Eng. 39 (2008) 137–142.
[7] Y.F. Guo, N.Q. Yan, S.J. Yang, P. Liu, J. Wang, Z. Qu, J.P. Jia, Conversion of elemental mercury with a novel membrane catalytic system at low temperature, J. Hazard. Mater. 213–214 (2012) 62–70.
[8] H.L. Li, C.Y. Wu, Y. Li, J.Y. Zhang, CeO_2–TiO_2 catalysts for catalytic oxidation of elemental mercury in low-rank coal combustion flue gas, Environ. Sci. Technol. 45 (2011) 7394–7400.
[9] H.K. Choi, S.H. Lee, S.S. Kim, The effect of activated carbon injection rate on the removal of elemental mercury in a particulate collector with fabric filters, Fuel Process. Technol. 90 (2009) 107–112.
[10] X.P. Fan, C.T. Li, G.M. Zeng, Z. Gao, L.H. Chen, W. Zhang, H.L. Gao, Removal of gas-phase element mercury by activated carbon fiber impregnated with CeO_2, Energy Fuels 24 (2010) 4250–4254.
[11] J.W. Wang, J.L. Yang, Z.Y. Liu, Gas-phase elemental mercury capture by a V_2O_5/AC catalyst, Fuel Process. Technol. 91 (2010) 676–680.
[12] S.S. Tao, C.T. Li, X.P. Fan, G.M. Zeng, P. Lu, X. Zhang, Q.B. Wen, W.W. Zhao, D.Q. Luo, C.Z. Fan, Activated coke impregnated with cerium chloride used for elemental mercury removal from simulated flue gas, Chem. Eng. J. 210 (2012) 547–556.
[13] M.H. Kim, S.W. Ham, J.B. Lee, Oxidation of gaseous elemental mercury by hydrochloric acid over $CuCl_2$/TiO_2-based catalysts in SCR process, Appl. Catal. B: Environ. 99 (2010) 272–278.
[14] C.Y. Wu, Y. Li, J.Y. Zhang, Superior activity of MnO_x–CeO_2/TiO_2 catalyst for catalytic oxidation of elemental mercury at low flue gas temperatures, Appl. Catal. B: Environ. 111–112 (2012) 381–388.
[15] Z.C. Li, L.Y. Wu, H.J. Liu, H.C. Lan, J.H. Qu, Improvement of aqueous mercury adsorption on activated coke by thiol-functionalization, Chem. Eng. J. 228 (2013) 925–934.
[16] Q.B. Wen, C.T. Li, Z.H. Cai, W. Zhang, H.L. Gao, L.H. Chen, G.M. Zeng, X. Shu, Y.P. Zhao, Study on activated carbon derived from sewage sludge for adsorption of gaseous formaldehyde, Bioresour. Technol. 102 (2011) 942–947.
[17] Z.M. Shen, J. Ma, Z.J. Mei, J.D. Zhang, Metal chlorides loaded on activated carbon to capture elemental mercury, J. Environ. Sci. 22 (2010) 1814–1819.

[18] G. Singh, I.P.S. Kapoor, S.M. Mannan, J. Kaur, Studies on energetic compounds: Part 8: thermolysis of Salts of HNO_3 and $HClO_4$, J. Hazard. Mater. 79 (2000) 1–18.
[19] D.L. Laudal, J.S. Thompson, J.H. Pavlish, L. Brickett, P. Chu, R.K. Srivastava, C. Lee, J.D. Kilgroe, Evaluation of mercury speciation at power plants using SCR and SCR NO_x control technologies, in: 3rd International Air Quality Conference, Arlington, VA, 2002.
[20] Y.X. Zhao, M.D. Mann, J.H. Pavlish, B.A. Mibeck, G.E. Dunham, E.S. Olson, Application of gold catalyst for mercury oxidation by chlorine, Environ. Sci. Technol. 40 (2006) 1603–1608.
[21] S.J. Lee, Y.C. Seo, J. Jurng, T.G. Lee, Removal of gas-phase elemental mercury by iodine- and chlorine-impregnated activated carbons, Atmos. Environ. 38 (2004) 4887–4893.
[22] X.Y. Hua, J.S. Zhou, Q. Li, Z.Y. Luo, K.F. Cen, Gas-phase elemental mercury removal by CeO_2 impregnated activated coke, Energy Fuels 24 (2010) 5426–5431.
[23] N.D. Hutson, B.C. Attwood, K.G. Scheckel, XAS and XPS characterization of mercury binding on brominated activated carbon, Environ. Sci. Technol. 41 (2007) 1747–1752.
[24] L. Ji, P.M. Sreekanth, P.G. Smirniotis, S.W. Thiel, N.G. Pinto, Manganese oxide/titania materials for removal of NO_x and elemental mercury from flue gas, Energy Fuels 22 (2008) 2299–2306.
[25] G.M. Veith, J. Nanda, L.H. Delmau, N.J. Dudney, Influence of lithium salts on the discharge chemistry of Li–air cells, J. Phys. Chem. Lett. 3 (2012) 1242–1247.
[26] A. Saraswat, L.K. Sharma, S. Singh, R. Singh, Electrochemical assisted synthesis and characterization of perchloric acid-doped aniline-functionalized copolymers, Synth. Met. 167 (2013) 31–36.
[27] A.F. Pérez-Cadenas, F.J. Maldonado-Hodar, C. Moreno-Castilla, On the nature of surface acid sites of chlorinated activated carbons, Carbon 41 (2003) 473–478.
[28] T.Y. Liu, H.C. Liao, C.C. Lin, S.H. Hu, S.Y. Chen, Biofunctional ZnO nanorod arrays grown on flexible substrates, Langmuir 22 (2006) 5804–5809.
[29] J.Y. Huang, Y.X. Shao, H.G. Huang, Y.H. Cai, Y.S. Ning, H.H. Tang, Q.P. Liu, S.F. Alshahateet, Y.M. Sun, G.Q. Xu, Binding mechanisms of methacrylic acid and methyl methacrylate on Si (1 1 1)-7 × 7 effect of substitution groups, J. Phys. Chem. B 109 (2005) 19831–19838.
[30] X. Gao, Y. Jiang, Y. Zhong, Z.Y. Luo, K. Cen, The activity and characterization of CeO_2–TiO_2 catalysts prepared by the sol–gel method for selective catalytic reduction of NO with NH_3, J. Hazard. Mater. 174 (2010) 734–739.
[31] Y. Eom, S.H. Jeon, T.A. Ngo, J. Kim, T.G. Lee, Heterogeneous mercury reaction on a selective catalytic reduction (SCR) catalyst, Catal. Lett. 121 (2007) 219–225.
[32] K. Tsuji, I. Shiraishi, Combined desulfurization, denitrification and reduction of air toxics using activated coke: 1. Activity of activated coke, Fuel 76 (1997) 549–553.
[33] S.A. Freunberger, Y. Chen, N.E. Drewett, L.J. Hardwick, F. Bardé, P.G. Bruce, The lithium–oxygen battery with ether-based electrolytes, Angew. Chem. Int. Ed. 50 (2011) 8609–8613.
[34] S.A. Freunberger, Y.H. Chen, Z.Q. Peng, J.M. Griffin, L.J. Hardwick, F. Bardé, P. Novák, P.G. Bruce, Reactions in the rechargeable lithium–O_2 battery with alkyl carbonate electrolytes, J. Am. Chem. Soc. 133 (2011) 8040–8047.
[35] D. Gorman-Lewis, S. Skanthakumar, M.P.s Jensen, S. Mekki, K.L. Nagy, L. Soderholm, FTIR characterization of amorphous uranyl-silicates, Chem. Geol. 253 (2008) 136–140.
[36] J. Yang, K.Q. Qiu, Preparation of activated carbon by chemical activation under vacuum, Environ. Sci. Technol. 43 (2009) 3385–3390.
[37] E. Vyhmeister, L. Reyes-Bozo, H. Valdés-González, J.-L. Salazar, A. Muscat, L.A. Estévez, D. Suleiman, F.T.I.R. In-situ, Experimental results in the silylation of low-k films with Hexamethyldisilazane dissolved in supercritical carbon dioxide, J. Supercrit. Fluids (2014).
[38] S.J. Huang, A.B. Walters, M.A. Vannice, Adsorption and decomposition of NO on lanthanum oxide, J. Catal. 192 (2000) 29–47.
[39] Z.Q. Tan, L.S. Sun, J. Xiang, H.C. Zeng, Z.H. Liu, S. Hu, J.R. Qiu, Gas-phase elemental mercury removal by novel carbon-based sorbents, Carbon 50 (2012) 362–371.
[40] G. Várhegyi, P. Szabó, F. Till, B. Zelei, M.J. Antal, X. Dai, TG, TG-MS, and FTIR characterization of high-yield biomass charcoals, Energy Fuels 12 (1998) 969–974.
[41] X.L. Zhang, ZhangF Y., S. Ding, Q.J. Huang, Y. Li., Effect of the surface properties of an activated coke on its desulphurization performance, Mining Sci. Technol. 19 (2009) 769–774.
[42] J.F. González, S. Román, C.M. González-García, J.V. Nabais, A.L. Ortiz, Porosity development in activated carbons prepared from walnut shells by carbon dioxide or steam activation, Ind. Eng. Chem. Res. 48 (2009) 7474–7481.
[43] A.J. Guo, Z.X. Wei, B. Zhao, K. Chen, D. Liu, Z.X. Wang, H. Song, Separation of toluene-insoluble solids in the slurry oil from a residual fluidized catalytic cracking unit: determination of the solid content and sequential selective separation of solid components, Energy Fuels 28 (2014) 3053–3065.
[44] A.C. Zhang, J. Xiang, L.S. Sun, S. Hu, P.S. Li, J.M. Shi, P. Fu, S. Su, Preparation, characterization, and application of modified chitosan sorbents for elemental mercury removal, Ind. Eng. Chem. Res. 48 (2009) 4980–4989.
[45] H.L. Li, Y. Li, C.Y. Wu, J.Y. Zhang, Oxidation and capture of elemental mercury over SiO_2–TiO_2–V_2O_5 catalysts in simulated low-rank coal combustion flue gas, Chem. Eng. J. 169 (2011) 186–193.
[46] Y. Li, P.D. Murphy, C.Y. Wu, K.W. Powers, J.C.J. Bonzongo, Development of silica/vanadia/titania catalysts for removal of elemental mercury from coal-combustion flue gas, Environ. Sci. Technol. 42 (2008) 5304–5309.
[47] W.Q. Xu, H.R. Wang, T.Y. Zhu, J.Y. Kuang, P.F. Jing, Mercury removal from coal combustion flue gas by modified fly ash, J. Environ. Sci. 25 (2013) 393–398.
[48] J.F. Li, N.Q. Yan, Z. Qu, S.H. Qiao, S.J. Yang, Y.F. Guo, P. Liu, J.P. Jia, Catalytic oxidation of elemental mercury over the modified catalyst Mn/α-Al_2O_3 at lower temperatures, Environ. Sci. Technol. 44 (2009) 426–431.
[49] Q. Wan, L. Duan, K.B. He, J.H. Li, Removal of gaseous elemental mercury over a CeO_2–WO_3/TiO_2 nanocomposite in simulated coal-fired flue gas, Chem. Eng. J. 170 (2011) 512–517.
[50] E.A. Morris, D.W. Kirk, C.Q. Jia, K. Morita, Roles of sulfuric acid in elemental mercury removal by activated carbon and sulfur-impregnated activated carbon, Environ. Sci. Technol. 46 (2012) 7905–7912.
[51] H.L. Li, C.Y. Wu, Y. Li, L.Q. Li, Y.C. Zhao, J.Y. Zhang, Impact of SO_2 on elemental mercury oxidation over CeO_2–TiO_2 catalyst, Chem. Eng. J. 219 (2013) 319–326.
[52] Y. Li, C.Y. Wu, Role of moisture in adsorption, photocatalytic oxidation, and reemission of elemental mercury on a SiO_2–TiO_2 nanocomposite, Environ. Sci. Technol. 40 (2006) 6444–6448.
[53] A. Murakami, M.A. Uddin, R. Ochiai, E. Sasaoka, S.J. Wu, Study of the mercury sorption mechanism on activated carbon in coal combustion flue gas by the temperature-programmed decomposition desorption technique, Energy Fuels 24 (2010) 4241–4249.